Revealing the differences in collision cross section values of small organic molecules acquired by different instrumental designs and prediction models

Revealing the differences in Collision Cross Section values of small organic molecules acquired by different instrumental designs and prediction models

Lidia Belova[1]*, Alberto Celma[2], Glenn Van Haesendonck[3], Filip Lemière[3], Juan Vicente Sancho[2], Adrian Covaci[1], Alexander L.N. van Nuijs[1], Lubertus Bijlsma[2]*

[1] Toxicological Centre, University of Antwerp, Universiteitsplein 1, 2610 Wilrijk, Belgium

[2] Environmental and Public Health Analytical Chemistry, Research Institute for Pesticides and Water, University Jaume I, Avinguda de Vicent Sos Baynat, 12006 Castelló, Spain

[3] Biomolecular & Analytical Mass Spectrometry (BAMS) group, University of Antwerp, Groenenborgerlaan 171, 2020 Antwerp, Belgium

*Corresponding authors:

Lidia Belova (ORCID: 0000-0001-7147-384X); E-mail: Lidia.Belova@uantwerpen.be; Toxicological Center, University of Antwerp, Universiteitsplein 1, 2610 Wilrijk, Belgium; Phone: +32 3 265 27 02

Lubertus Bijlsma (ORCID: 0000-0001-7005-8775); E-mail: bijlsma@uji.es ; Environmental and Public Health Analytical Chemistry, Research Institute for Pesticides and Water, University Jaume I, Avinguda de Vicent Sos Baynat, 12006 Castelló, Spain

ABSTRACT

The number of open access databases containing experimental and predicted collision cross section (CCS) values is rising and leads to their increased use for compound identification. However, the reproducibility of reference values with different instrumental designs and the comparison between predicted and experimental CCS values is still under evaluation.

This study compared experimental CCS values of 56 small molecules (Contaminants of Emerging Concern) acquired by both drift tube (DT) and travelling wave (TW) ion mobility mass spectrometry (IM-MS). The TWIM-MS included two instrumental designs (Synapt G2 and VION). The experimental $^{TW}CCS_{N2}$ values obtained by the TWIM-MS systems showed absolute percent errors (APEs) < 2% in comparison to experimental DTIMS data, indicating a good correlation between the datasets. Furthermore, $^{TW}CCS_{N2}$ values of $[M-H]^-$ ions presented the lowest APEs. An influence of the compound class on APEs was observed.

The applicability of prediction models based on artificial neural networks (ANN) and multivariate adaptive regression splines (MARS), both built using TWIM-MS data, was investigated for the first time for the prediction of $^{DT}CCS_{N2}$ values. For $[M+H]^+$ and $[M-H]^-$ ions, the 95th percentile confidence intervals of observed APEs were comparable to values reported for both models indicating a good applicability for DTIMS predictions.

For the prediction of $^{DT}CCS_{N2}$ values of $[M+Na]^+$ ions, the MARS based model provided the best results with 73.9% of the ions showing APEs below the threshold reported for $[M+Na]^+$. Finally, recommendations for database transfer and applications of prediction models for future DTIMS studies are made.

KEYWORDS

Travelling wave ion mobility separation; drift tube ion mobility separation; compounds of emerging concern; quality assurance guidelines; CCS comparison; CCS database

1. INTRODUCTION

Ion mobility spectrometry (IMS) has demonstrated to be a powerful additional technique for compound identification within target, suspect and non-target screening studies in various research fields [1-4]. IMS allows a conformational separation of ions based on their gaseous mobility through a drift gas (e.g., N_2 or He) under the influence of an electric field. Hence, the hyphenation of IMS with gas or liquid chromatography (GC or LC) and high resolution mass spectrometry (HRMS) provides an additional separation dimension [5, 6]. Moreover, the measured drift times can be converted into collision cross section (CCS) values which describe the rotationally averaged surface of ions for which collision with the buffer gas occur [7].

Drift tube IMS (DTIMS) and travelling wave IMS (TWIMS) are both designed as dispersive techniques, allowing all ions to pass through for subsequent analysis and are the most commonly applied designs [8]. DTIMS separates ions in a low uniform electric field (typically 5–100 V/cm). This permits a direct calculation of CCS values from the measured arrival times (t_A; i.e., the time it takes the ion to travel from the entrance of the drift tube to the detector) without the use of external calibrants provided that various measurements are conducted applying different electric fields[9, 10]. This is commonly referred to as the stepped field calibration method. On the contrary, the single field calibration method allows the calculation of CCS values directly from the t_A measured at a single electric field based on a set of calibrant compounds with previously known CCS values [11].

TWIMS instruments operate applying both a radio frequency (RF) and a pulsed differential current (DC) voltage to the ion mobility cell. While the DC voltage ensures the axial movement of ions, the RF voltage allows radial ion confinement through periodically alternating between positive and negative polarities [12]. This creates an electric field in the form of a wave whose height and velocity influence the separation of ions [8]. For TWIMS measurements, a direct calculation of CCS values from the measured drift times is not possible since the applied electric field is not uniform. However, CCS values can be calculated based on a set of predefined calibrants whose reference DTIMS derived CCS values are available. This approach has been described in detail in previous studies [13, 14]. Additionally, it has been shown that a structural similarity between calibrants and analytes is essential to ensure reliable CCS calculations [15, 16].

Since IMS allows the separation of ions of interest from coeluting matrix components, CCS values are independent of potential matrix effects or the applied chromatographic conditions[9, 17]. Hence, they can serve as an additional identification parameter in feature annotation and compound identification leading to a reduction of false positive identifications [18, 19]. Furthermore, IMS has the potential to separate isomeric and isobaric compounds. As shown in previous studies, this is especially relevant if the isomeric compounds have similar retention times (RT) or fragmentation

patterns which do not allow their unequivocal identification [19-21]. Additionally, when implemented within data-independent acquisition (DIA) workflows, IMS facilitates the removal of spectral interferences as these show different drift times than the compound of interest and its corresponding fragments. This leads to cleaner mass spectra further improving compound annotation [19, 22].

The implementation of IMS in suspect and non-target screening studies on small molecules has been discussed in detail in previous studies [21, 23-25]. Thereby, CCS values of signals of interest are matched against CCS values of reference standards, scientific literature or open-source libraries [26-28], including several online platforms which contain curated CCS datasets from various sources [29-31]. Moreover, the inclusion of ion mobility data in widely adopted confidence levels for identification of small molecules in environmental studies, including a cut-off value of 2% for the deviation between experimental and reference CCS values, has been proposed recently [21].

However, the high number of compounds monitored in suspect and non-target screening studies and the unavailability of reference standards lead to a lack of reference CCS values for many suspects, currently limiting the use of CCS for compound identification. This data gap can in theory be filled through the *in-silico* prediction of CCS values. Various prediction tools for different compound classes are available in the literature [31-36]. These tools are based on experimental CCS values and apply different predictions models including machine-learning algorithms [31], such as artificial neural networks (ANN) [36]. Prediction tools have demonstrated good prediction accuracies making them a valuable addition for suspect and non-target screening studies [37, 38].

Despite the high efforts put into CCS database building and the development of prediction models, CCS values remain an estimated empirical value which is influenced by the instrumental design and the applied calibration approach. The uncertainty of IMS-MS measurements has been assessed in detail previously [10, 39]. Several studies have investigated the inter-laboratory and inter-instrumental reproducibility of CCS measurements [10, 14, 40]. Stow et al. reported a relative standard deviation (RSD) of 0.29% for stepped-field measurements of $^{DT}CCS_{N2}$ values in three different laboratories of which all applied DTIMS [10]. Hinnenkamp et al. compared CCS values acquired using TWIMS and DTIMS instruments for a set of 124 compounds and reported absolute errors of < 1% for 66%; between 1-2% for 27% and >2% for 7% of the proton adducts of the investigated compounds [14].

Based on a set of 56 contaminants of emerging concern (CECs) and their metabolites, the present study aimed to further investigate the reproducibility of CCS values acquired on DTIMS and two TWIMS instruments applying different calibration approaches and evaluating factors potentially causing deviations. This work also included the investigation of CCS values for deprotonated ion

which were not present in the above mentioned $^{DT}CCS_{N2}$ and $^{TW}CCS_{N2}$ comparison [14]. Furthermore, DTIMS derived CCS values were compared with predicted values employing two prediction models built with TWIMS derived data, namely an ANN based prediction tool and a Multiple Adaptive Regression Splines (MARS) prediction model previously developed by Bijlsma et al. [36] and by Celma et al. [41], respectively. Finally, we also aimed to estimate the cut-off values for database transfer from one instrumental design to another and the applicability of TWIMS-based prediction models for DTIMS measurements. This study adds to the detailed recommendations for the reporting of experimental IMS measurements published by Gabelica et al. [9] and it proposes the minimum and most relevant parameters to be reported for open-access databases of predicted CCS values. These recommendations will further contribute to a more uniform reporting of IMS data and will allow potential users to critically review and assess comparability with their own data. The presented results are expected to serve as a valuable additional guideline for the implementation of IMS in future studies on small molecule identifications.

2. Materials and Methods

2.1 Selection of standards

A set of 56 compounds, including five compound classes: triazoles, organophosphate flame retardants (OPs), plasticizers and metabolites of the latter two, were selected for this comparison study. The selection of compounds was based on the following considerations: i) inclusion of various compound classes, incl. metabolites, ii) availability of ions in both ionization polarities, and iii) availability of reference standards, shared between laboratories. The selected compounds including their name, abbreviation, molecular formula, structure, SMILES, monoisotopic mass, InChi and InChiKey are summarized in **Table S1**. The sources from which the reference standards were acquired can be found in the study from Belova et al. [20].

2.2 IMS measurements

2.2.1 DTIMS measurements

The $^{DT}CCS_{N2}$ values of the compounds included in this study were previously reported[20] and are summarized in **Table S1**. In the corresponding publication, a detailed description of the method used for the acquisition of $^{DT}CCS_{N2}$ values can be found. In brief, all $^{DT}CCS_{N2}$ values were acquired on an Agilent 6560 DTIM-QTOF applying the single-field calibration method. For CCS calibration, the ESI low-concentration tune mix (Agilent Technologies, Santa Clara, USA) was used. The reference $^{DT}CCS_{N2}$ values of the tune mix ions were acquired by Stow et al. on a reference DTIMS system [10] and are summarized in **Table S2** and **Table S3**. Each standard was introduced in the DTIMS-QTOF by

direct injection at 1 ng/µL. For each standard, five measurements were conducted. The average $^{DT}CCS_{N2}$ value and (relative) standard deviations are reported (**Table S1**).

2.2.2 TWIMS measurements (VION)

The first set of $^{TW}CCS_{N2}$ values was acquired on a VION IMS-QTOF mass spectrometer (Waters, Milford, MA, USA), equipped with an electrospray ionization (ESI) interface operating in positive and negative ionization modes. The ionization source was operated applying the following voltages: capillary voltage of 0.8 kV; cone voltage 40 V with desolvation temperature set to 550 °C, and the source temperature to 120 °C. Nitrogen (N_2) was used as the drying gas and nebulizing gas. The cone gas flow was 250 L/h and desolvation gas flow of 1000 L/h. MS data were acquired in $HDMS^E$ mode, over the range *m/z* 50-1000, with N_2 as the drift gas, an IMS wave velocity of 250 m s^{-1} and wave height ramp of 20-50 V. Leucine enkephalin (*m/z* 556.2766 and *m/z* 554.2620) was used for mass correction in positive and negative ionization modes, respectively. Two independent scans with different collision energies were acquired during the run: a collision energy of 6 eV for low energy (LE) and a ramp of 28-56 eV for high energy (HE). A scan time of 0.3 s was set in both LE and HE functions. Nitrogen (≥ 99.999%) was used as collision-induced dissociation (CID) gas. All data were examined using an in-house built accurate mass screening workflow within the UNIFI platform (version 1.9.4) from Waters Corporation. More details about the methodology followed can be found elsewhere [21].

2.2.3 TWIMS measurements (Synapt G2)

The second set of TWIMS derived $^{TW}CCS_{N2}$ values was acquired on a Synapt G2 HD mass spectrometer (Waters, Milford, MA, USA) equipped with a nano-electrospray ionization source. The ionization source was operated applying the following voltages: capillary voltage 2.5 kV, extraction cone 5 V; sample cone 35 V; trap collision energy 4.0 V; transfer collision energy 4.0 V; trap DC bias 35 V. The wave velocity was set to 1000 m/s at a constant wave height of 40 V. The gas pressures within the instrument were set as follows: desolvation gas flow 35 L/h (at a temperature of 150 ˚C); trap gas flow 0.4 mL/min; IMS gas flow 90 mL/min; helium cell gas flow 180 mL/min. For sample infusion, in-house pulled and gold-coated borosilicate capillaries were used.

For the positive ionization mode, calibration compounds proposed by Campuzano et al. were used to calculate $^{TW}CCS_{N2}$ values[42]. For the negative ionization mode, poly-DL-alanine was chosen for CCS calibration based on the data published by Bush et al. [43]. The molecular formulae, SMILES, CAS numbers, sources of purchase of the reference standard and reference CCS values of the calibrants and QA compounds are summarized in **Table S4**.

Solutions of the calibration compounds were prepared in water/methanol (50/50; v/v) containing 0.1% formic acid at concentrations between 0.12 ng/µL and 0.61 ng/µL (10^{-6} M). Solutions of analytes and quality assurance (QA) compounds were prepared at 1ng/µL in water/acetonitrile (50/50; v/v) containing 0.1% formic acid. To all infused solutions (both calibrants and analytes) leucine-enkephalin was spiked prior to infusion at a concentration of 5 ng/µL to be used as a lock-mass for mass calibration within data analysis. For the measurement of $^{TW}CCS_{N2}$ values, all analytes were infused in triplicate. The instrument was operated using the MassLynx software (version 4.1 SCN 781). After recalibration based on the added lock-mass of leucine-enkephalin, extracted ion mobilograms for each calibrant were obtained to allow establishing individual drift time values. The latter were then used to obtain the calibration curves for positive and negative ionization modes (Figure S1) that enable the calculation of $^{TW}CCS_{N2}$ values. The detailed workflow for $^{TW}CCS_{N2}$ calculations has been described in detail in previous studies [13, 14].

2.3 Quality assurance (QA) measures

Within each instrumental design used in this study, QA measures were implemented. For DTIMS, the acquisition of $^{DT}CCS_{N2}$ values of nine QA compounds was conducted within each analytical batch. For these QA compounds reference $^{DT}CCS_{N2}$ values acquired on a reference DTIMS system were available [10]. The QA measures and results of the DTIMS measurements have been described in detail previously [20].

For $^{TW}CCS_{N2}$ on the VION system, a set of nine QA compounds included in the System Suitability Test (SST) mix provided by the manufacturer was used to evaluate the accuracy and performance of the instrument as well as to ensure the reproducibility of the measurements. The molecular formulae, SMILES and reference CCS values of the Vion QA compounds are summarized in **Table S5**.

Terfenadine, sulfaguanidine, sulfadimethoxine and caffeine were used as QA compounds for measurements on the Synapt G2 system in positive and sulfaguanidine and sulfadimethoxine in negative ionization mode, respectively. The selection of QA compounds was based on the compounds included in the SST mix used for the TWIMS measurements on the Waters VION instrument and aimed to serve as a QA measure for measurement reproducibility between the two TWIMS set-ups used in this study. Reference CCS values of the QA compounds were provided by the manufacturer (**Table S4**).

2.4 CCS predictions

2.4.1 Artificial Neural Network (ANN) based prediction model

ANN predictions of CCS values were made using Alyuda NeuroIntelligence 2.2 (Cupertino, CA) by applying a predictor previously developed and optimized [36]. Briefly, eight relevant molecular descriptors of the selected compounds were obtained from an Online Chemical Database (www.ochem.eu) [44]. The ANN predictor, trained by means of a database of empirical $^{TW}CCS_{N2}$ values for 205 protonated small molecules, consisted of a neural network structured in three layers with 8-2-8-1 distribution. The relative error of CCS prediction was within 6% for the 95th percentile of all values for protonated ions and 8.7% for sodium adducts. Further details on the methodology can be found elsewhere [36].

2.4.2 Multivariate Adaptive Regression Splines (MARS) based prediction model

CCS predictions using Multivariate Adaptive Regression Splines were performed as follows: the statistical model was trained with empirical $^{TW}CCS_{N2}$ values of a total number of 470 protonated ions and a set of 7 molecular descriptors obtained from the Online Chemical Database (www.ochem.eu) [44]. The optimized model yielded an accuracy of 4.0% and 5.9% for the 95th percentile of predicted CCS values of protonated and deprotonated ions, respectively. Moreover, an additional and unique model was developed for predicting CCS values of sodium adducts obtaining an accuracy of 5.3% (95th percentile). More details of these prediction models can be found elsewhere [41].

3. RESULTS AND DISCUSSION

3.1 Quality control and quality assurance results.

Figure S2 summarizes the QA approaches implemented in the DTIMS and TWIMS measurements. This approach used within DTIMS measurements allowed the comparison with reference values obtained using the same instrumental design leading to low percent errors (PE) (all < 0.2%) [20]. This confirmed the reproducibility and accuracy of the DTIMS system used in this study.

Within the acquisition of $^{TW}CCS_{N2}$ values on the TWIMS VION system, the analysis of an SST mixture containing nine compounds was included (**Table S5**). For these compounds, reference CCS values were provided by the manufacturer. As it is the case for other reference CCS values used for TWIMS measurements [42, 43], the provided CCS values were derived from DTIMS based measurements conducted on a modified Synapt G2 instrument. The VION instrument performance was satisfactory based on a 2% threshold for the deviation between expected and empirical CCS values.

The selection of suitable QA compounds for $^{TW}CCS_{N2}$ measurements on the Synapt instrument aimed to show an overlap with the SST compounds used on the VION system to investigate the reproducibility between the two TWIMS set-ups. Nevertheless, the QA approaches of both TWIMS systems must be viewed critically as in both cases experimental $^{TW}CCS_{N2}$ values are compared with

DTIMS data. Thus, this approach represents rather a comparison of measurements between the different TWIMS set-ups than a fully independent QA approach.

The results of the Synapt G2 QA measurements are summarized in **Table S6**. Average absolute percent errors (APEs) of 1.42% and 0.60% were observed for measurements in positive and negative ionization polarities, respectively. Both values fall within the 2% cut-off for the evaluation of SST measurements on the VION system and indicate a good reproducibility between the two TWIMS set-ups. Nevertheless, two QA compounds (sulfaguanidine and caffeine) showed deviations slightly above 2% in positive mode. These deviations must be interpreted critically as they do not indicate a poor instrumental performance, but rather a deviation between experimental TWIMS derived CCS values and the DTIMS based reference values. This will further be investigated in this study. The observed APEs can also be caused by the low CCS values observed for these compounds (CCS < 150 $Å^2$) whereby even small deviations in measured t_A lead to high percent errors.

3.2 Selection of reference CCS values for further comparisons

The comparison of experimental DTIMS and TWIMS derived CCS values was based on a set of 56 standards including five compound classes: triazoles, organophosphate flame retardants (OPs), plasticizers and metabolites of the latter two. Data on proton and sodium adducts, as well as deprotonated ions were included. In general, the comparison between sets of CCS values is commonly conducted through reporting the observed (absolute) percent errors [14, 40, 45]. When applying this approach for the present study, the question about which set of CCS values to use as the reference set arose. Since none of the datasets was acquired with DTIMS stepped-field calibration, none of the datasets can be viewed as a calibrant-independent reference. To validate the two prediction models applied in this study, predicted CCS values have already been compared with the corresponding experimental TWIMS datasets [36]. Therefore, the use of the $^{TW}CCS_{N2}$ dataset as reference would reproduce this approach and exclude the available $^{DT}CCS_{N2}$ values from the comparison. Additionally, the choice of the reference dataset should allow the comparison of observed deviations between the different datasets. Therefore, $^{DT}CCS_{N2}$ values were used as reference for all calculations included in this study. Even though these values were acquired using the single-field calibration approach and thus required calibrants, the influence of the selected calibrants on the reproducibility of measurements was expected to be lower than for TWIMS calculations [10, 43]. Ultimately, the following equation was applied for the calculation of percent errors between DTIMS and TWIMS derived or predicted CCS values:

$$\text{Error } [\%] = \left(\frac{CCS_{TWIMS/pred} - CCS_{DTIMS}}{CCS_{DTIMS}}\right) \cdot 100 \quad (1)$$

3.3 Comparison of experimental $^{TW}CCS_{N2}$ and $^{DT}CCS_{N2}$ values

For the 56 compounds, 108 $^{DT}CCS_{N2}$ values were included in the DTIMS reference database as several of the compounds were detected both as proton and sodium adducts and/or in both ionization polarities. A total of 29 $[M+H]^+$ ions, 46 $[M+Na]^+$ ions and 33 $[M-H]^-$ ions were observed (**Table S1**). The acquisition of $^{TW}CCS_{N2}$ values on the TWIMS VION instrument allowed the detection of a total of 94 ions which corresponded to 50 compounds available for the comparison (**Table S7**). Thus, six compounds were not detectable on the TWIMS VION set-up which was assumed to be caused by differences in ionization source parameters and geometries leading to differences in ionization efficiencies. The 94 detected ions included 22 $[M+H]^+$ ions and 40 $[M+Na]^+$ ions, as well as 32 $[M-H]^-$ ions. Measurements on the Synapt G2 system yielded a total of 97 $^{TW}CCS_{N2}$ values which corresponded to 54 compounds detected (**Table S7**). Two compounds, tris(2-ethylhexyl)trimellitate and bisphenol A bis(diphenyl phosphate), were not detected on the Synapt G2 and VION instruments. Hence, for a total of 50 compounds, at least one CCS value was available from each of the instrumental set-ups. Within the 97 ions detected on the Synapt G2 system, 23 $[M+H]^+$, 41 $[M+Na]^+$ and 33 $[M-H]^-$ ions were included.

As displayed in **Figure S3**, 83% and 82% of all included ions showed APEss < 2% for the comparison of DTIMS data with the VION and Synapt systems, respectively. For protonated adducts, 64% (VION) and 57% (Synapt) of the observed ions had APEs < 2%. For the sodium adducts, the observed percentages of ions with APEs < 2% were 83% and 93% for the VION and Synapt systems, respectively. Deprotonated ions showed the lowest APEs within the comparison between TWIMS and DTIMS systems. For both VION and Synapt G2 systems, only one $[M-H]^-$ ion showed an APE > 2% resulting in 97% of $[M-H]^-$ ions with APEs < 2%.

For a more detailed comparison, linear correlations between experimental DTIMS and TWIMS datasets were investigated. **Figure S4** shows the correlations observed between $^{DT}CCS_{N2}$ and $^{TW}CCS_{N2}$ values acquired on the VION (**Figure S4A**) and Synapt (**Figure S4B**) systems.

For both TWIMS systems, high correlation coefficients (R^2) were observed indicating a good linear correlation between $^{DT}CCS_{N2}$ and $^{TW}CCS_{N2}$ datasets. However, the R^2 of 0.9889 observed for VION data was slightly lower than for Synapt data (R^2 = 0.9929). Based on a visual inspection of the linear plots, the higher correlation coefficient observed for Synapt data is assumed to be mainly caused by the lower deviations from the trendline observed for CCS values of plasticizer metabolites in comparison with VION derived data. Additionally, interpolated regression lines indicate that $^{TW}CCS_{N2}$ datasets can be correlated to $^{DT}CCS_{N2}$ datasets with a slope close to 1 (0.9999 for Vion and 1.0180 for Synapt). This indicates that deviations between $^{DT}CCS_{N2}$ and $^{TW}CCS_{N2}$ are negligible, and data can be well compared. In order to investigate CCS deviations more in detail and distinguish between ionization polarities

and ion species, combined violin and box plots of the observed percent errors were created for each dataset (**Figure 1**).

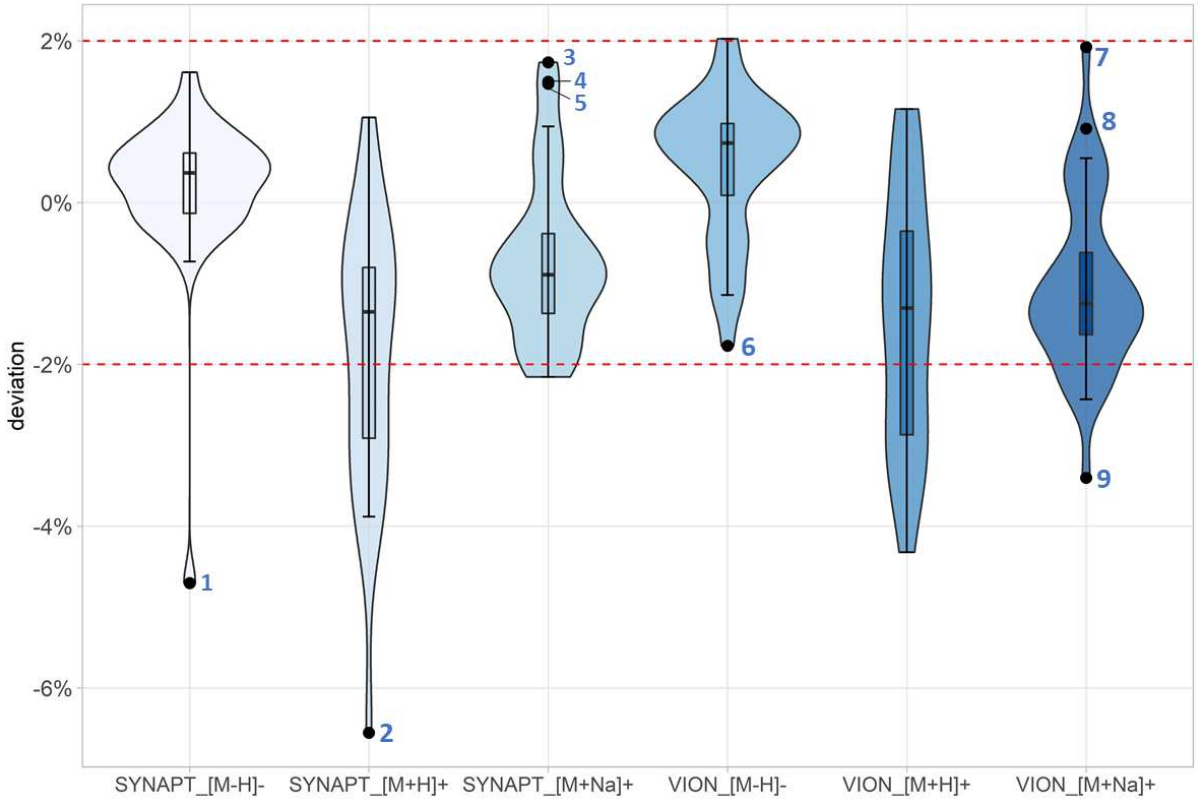

Figure 1: Combined box and violin plots of the error distributions observed when comparing $^{DT}CCSN_2$ values with experimental $^{TW}CCS_{N2}$ values *i.e.,* Synapt and Vion acquired in either positive or negative ionization mode. A distinction is made between proton and sodium adducts. The outliers observed for each dataset are numbered as follows: 1: BTR, 2: 5Cl-BTR, 3: DIDP, 4: DINCH, 5: DIDP, 6: pOH-TPHP, 7: EHDPHP, 8: MiBP, 9: TDCIPP. The full names of the mentioned compounds can be found in Table S3. A deviation of +/- 2% is indicated with a red dashed line.

Figure 1 shows the combined violin and boxplots of error distributions observed for experimental TWIMS data acquired in either negative or positive ionization mode. Additionally, bar charts in **Figures S5** and **S6** summarize the percent errors observed for each ion of each individual compound. A threshold of 2% for the use of reference CCS values for compound identification was proposed, within a recent study [21]. To evaluate the applicability of this threshold for databases acquired with different instrumental designs, all APEs observed in this study were compared to this cut-off value. For $[M+H]^+$, both the Synapt G2 and VION systems show comparable error distributions with mean values of -1.9% and -1.4% and interquartile ranges (IQR) of 2.1% and 2.5%, respectively. The negative mean values indicate a clear off-set between DTIMS and TWIMS derived data as most $^{TW}CCS_{N2}$ values of proton adducts where lower than the corresponding $^{DT}CCS_{N2}$ values. Except for the VION derived $^{TW}CCS_{N2}$ value of tris(1,3-dichloro-2-propyl) phosphate (TDCIPP) with a deviation of -2.84%, all other deviating $^{TW}CCS_{N2}$ values of $[M+H]^+$ ions belonged either to the group of triazoles or organophosphate flame retardants (and metabolites) carrying at least two phenyl moieties. Triazoles

represent the class with the lowest *m/z* values (*m/z* 118 – 154) investigated in the study. Low *m/z* values result in lower CCS values for which even small absolute deviations can lead to high percentual errors. As it was previously observed for diphenyl phthalate (DPP) [20], aromatic substitutes are assumed to lead to more compact ions resulting in lower $^{DT}CCS_{N2}$ values. The observed deviations of TWIMS data lead to the assumption that this effect has a higher influence within DTIMS measurements, indicating differing molecular conformations of the described compounds between TWIMS and DTIMS systems.

Interestingly, the error distributions observed for $[M+Na]^+$ show a smaller spread in comparison to the protonated ions. The deviations calculated for $[M+Na]^+$ showed mean values of -0.7% and -1.0% and IQRs of 1.0% and 1.0% for the Synapt and VION systems, respectively. A study by Hinnenkamp et al. reported slightly higher percent errors for sodium adducts in comparison to protonated ions: 87% of the included $[M+Na]^+$ ions showed APEs < 2% while this percentage was 93% for $[M+H]^+$ [14]. This was assumed to be caused by the fact that sodium adducts were not included in the ions used as calibrants for TWIMS measurements. However, these observations were not reproduced in this study which might be caused by different compound classes or sample sizes included in the two studies. Again, a negative off-set between $^{TW}CCS_{N2}$ and $^{DT}CCS_{N2}$ values was observed, as most $^{TW}CCS_{N2}$ values of $[M+Na]^+$ ions were lower than the corresponding DTIMS values (**Figures S4** and **S5**). From the VION derived $^{TW}CCS_{N2}$ values of $[M+Na]^+$ ions, for seven values an APE > 2% was observed. Again, four of the seven values belonged to organophosphate flame retardants (OPs) and their metabolites carrying phenyl moieties. From the Synapt derived $^{TW}CCS_{N2}$ values of $[M+Na]^+$ ions, three values showed a APE > 2%. All of these deviating values overlapped with the deviating VION derived values and included two OPs carrying phenyl moieties (triphenyl phosphate and diphenylcresyl phosphate). Except for mono-(3-carboxypropyl) phthalate (PE of -2.2%), all remaining deviating $^{TW}CCS_{N2}$ values of $[M+Na]^+$ ions belong to the group of halogenated OPs and metabolites. Here, an influence of the applied calibrants is assumed. While the calibrants used for DTIMS measurements included several halogenated compounds (Tables **S2** and **S3**), this was not the case for neither the Synapt nor the VION calibrations possibly leading to the observed high deviations for halogenated compounds. The latter was confirmed by the fact that the $^{TW}CCS_{N2}$ values of the $[M+H]^+$ ion of 5-chlorobenzotriazole (5Cl-BTR) showed the highest deviation of all $[M+H]^+$ ions for both the VION and Synapt systems (outlier nr. 2 in **Figure 1**). However, further investigations are needed to confirm these effects for larger sample sizes and wider *m/z* ranges.

Within the Synapt dataset of $[M+Na]^+$ ions, three outliers (nr. 3-5 in **Figure 1**) with higher $^{TW}CCS_{N2}$ values in comparison to the corresponding $^{DT}CCS_{N2}$ values were identified. These values derived from diisodecyl phthalate (DIDP), diisononyl phthalate (DINP) and diisononyl cyclohexane 1,2-dicarboxylic

371 acid (DINCH). For two of these compounds (DIDP and DINCH), the $^{DT}CCS_{N2}$ values of sodium adducts
372 were lower than the corresponding values of protonated adducts which was in contrast to the trend
373 observed for most other compounds included in the $^{DT}CCS_{N2}$ database[20]. This observation was not
374 reproduced for the Synapt derived $^{TW}CCS_{N2}$ values leading to the assumption of different ion
375 conformations being observed between the TWIMS and DTIMS systems due to slight differences in
376 ionization processes. Alternatively, the fact that the used DIDP and DINCH standards represented
377 mixtures of isomers could also lead to the described observations.

378 During the comparison of datasets acquired in positive ionization polarity, an unexpectedly high
379 error (15.31%) was observed for the proton adduct of bis(1,3-dichloro-2-propyl) phosphate
380 (BDCIPP). A close reinvestigation of the DTIMS raw data indicated that the high $^{DT}CCS_{N2}$ value was
381 caused by an impurity of tris(1,3-dichloro-2-propyl) phosphate (TDCIPP) in the BDCIPP standard from
382 which latter was formed through post drift tube fragmentation. This led to a signal for BDCIPP which
383 showed the same drift time as tris(1,3-dichloro-2-propyl) phosphate leading to the high CCS value.
384 Within the plots of *m/z* versus CCS values which were created from the DTIMS dataset[20], the
385 incorrectly assigned CCS values had not shown a clear deviation from the observed trendlines. Thus,
386 the incorrect assignment could not be identified prior to the comparison conducted in this study.
387 The BDCIPP standard was reanalyzed using the same workflow[20]. These measurements lead to a
388 $^{DT}CCS_{N2}$ value 157.35 $Å^2$ and a lower observed deviation (-1.5 %). This value was used for all
389 comparisons described above and was added to the previously published DTIMS database to correct
390 the incorrect assignment.

391 For the dataset acquired in negative ionization polarity, the observed deviations show a lower
392 spread compared to the positive ionization mode. This reflects in the low IQRs of 0.7% and 0.9% for
393 Synapt and VION datasets, respectively. Within the Synapt G2 dataset, all APEs of negatively charged
394 ions were < 2%, except for the outlier indicated in **Figure 1** (outlier nr. 1, $[M-H]^-$ ion of benzotriazole).
395 For the VION dataset, one out of 32 CCS values of $[M-H]^-$ ions showed an APE of > 2% ($[M-H]^-$ ion of
396 2,4-di-(2-ethylhexyl) trimellitate). These observations indicate a high reproducibility of CCS values of
397 $[M-H]^-$ ions between different instrumental set-ups. The observed high reproducibility might be due
398 to the fact that OPs and their metabolites (for which high deviations were observed in positive
399 ionization polarity) were not included, since these compounds were not detected in negative
400 ionization polarity. Additionally, an opposite trend in comparison to data obtained in positive
401 ionization polarity was observed: both datasets showed a positive median error indicating a positive
402 off-set between TWIMS and DTIMS data. The included compound classes which differed between
403 the datasets might have an influence on these effects.

Good correlations were observed between DTIMS and TWIMS derived CCS values. Nevertheless, a few compounds showed high deviations of up to -4.3% and -6.6%. Several potential factors which might cause the high deviations could be identified and must be considered when interpreting the quality and reliability of the presented dataset. Firstly, an influence of the compound class can be assumed as most of the highly deviating values derived from a particular class (OPs and their metabolites carrying at least two phenyl substituents). These effects might be traced back to differences in ion conformations between DTIMS and TWIMS systems for certain classes. Secondly, an effect of the applied calibration approach on CCS deviations is considered possible. Several previous studies have characterized the influence of the calibrants applied for TWIMS measurements and addressed the advantage of a match in compound class and charge state between calibrants and analytes. However, most of these studies focused on proteomic and lipidomic applications, which means that only a limited amount of studies including small molecules applications can be found [15, 16, 46]. Recently, a study assessed the influence of different calibration approaches on TWIMS measurements of steroids evaluating and comparing the observed bias. Additionally, a new set of reference DTIMS derived CCS values for TWIMS calibration was proposed whose implementation improved the reproducibility of CCS measurements on different instrumental set-ups [47]. These observations highlight the need of similar evaluations of different calibration approaches for the analysis of CECs and a potential implementation of the newly proposed sets of reference CCS values. A critical manual evaluation of the calibration approaches applied for the compilation of TWIMS derived databases thus remains crucial before database implementation for different instrumental designs and/or calibration approaches. Lastly, the described limitations confirm that CCS values represent empirical measurements which are influenced by several factors and do not allow the establishment of a “true CCS value”. It is recommended to assess potential deviations based on a subset of reference standards of the class of interest prior to applying a database acquired with a different instrumental design. Subsequently, the cut-off value of 2% which has been proposed previously[21] might need to be adjusted for databases deriving from different instrumental designs or different calibration approaches.

3.4 Comparison of predicted CCS and experimental $^{DT}CCS_{N2}$ values

The experimental $^{DT}CCS_{N2}$ values were compared with predicted datasets which derived from two different prediction models, namely an ANN and a MARS based model [36, 41]. Both models were built using experimental TWIMS derived CCS values. To the best of our knowledge, this is the first study investigating the capabilities of these models in predicting CCS values for DTIMS measurements.

During the development of the ANN based prediction model, an APE < 6% was observed for 95% of the protonated ions when comparing predicted with experimental $^{TW}CCS_{N2}$ values. To be able to compare these observations, the same threshold (6%) was applied to access the deviations of ANN based predicted CCS values (further referred to as CCS_{ANN}) of $[M+H]^+$ ions presented here. A 6% threshold was also used to access deviations of $[M-H]^-$ ions, even though it must be noted that the ANN based model was built using $[M+H]^+$ data, but not evaluated for $[M-H]^-$ ions within its development. For $[M+Na]^+$ ions, an APE of 8.7% was reported for the 95th percentile confidence interval [36]. This higher values is caused by the fact that the ANN based prediction model has been developed without the inclusion of $[M+Na]^+$ ions in the training, validation and blind datasets [36]. On the contrary to the $[M-H]^-$ ions, $[M+Na]^+$ data has been evaluated within its development. Hence, a threshold of 8.7% was applied for $[M+Na]^+$ ions as higher APEs can be assumed for this ion species.

Figure 2 shows the combined violin and boxplots of the error distributions observed for predicted CCS values differentiating between prediction models and ion species. For the linear correlation between $^{DT}CCS_{N2}$ and CCS_{ANN} values, a correlation coefficient of R^2 = 0.9305 and a slope of 0.9753 were observed (see **Figure S7A**). For $[M+H]^+$ ions, the ANN based model showed a median APE of -1.8% and an IQR of 1.6%. Due to the small IQR (in comparison to other ion species) which influences the upper and lower fence (defined as the Q_3/Q_1 +/- 1.5 x IQR), several outliers were observed (see **Figure 2**). Similar to the comparison of experimental $^{DT}CCS_{N2}$ and $^{TW}CCS_{N2}$ values, all observed outliers belonged to either OPs (and metabolites) with at least two aromatic moieties or low-mass (halogenated) triazoles. Nevertheless, most of the observed outliers fall within the threshold of ± 6% resulting in 93.1% of the CCS_{ANN} values showing an APE < 6%. Comparable results were obtained for CCS_{ANN} values of $[M-H]^-$ ions of which 93.9% showed APEs < 6% with only two values exceeding this threshold (CCS_{ANN} of mono(2-ethylhexyl) terephthalate and mono(2-ethyl-5-hydroxyhexyl) terephthalate). Therefore, for $[M-H]^-$ and $[M+H]^+$, it can be concluded that the ANN based prediction model can successfully be applied for DTIMS measurements of small molecules structurally similar to the compound classes investigated here. Again, the deviations observed for some classes point out the necessity of evaluating the applicability of the model based on a subset of reference standards.

CCS_{ANN} values of $[M+Na]^+$ ions show the highest APE with a median value of -3.7% and an IQR of 6.8%. From the 46 $[M+Na]^+$ ions included in the comparison, 80.4 % showed an APE below the applied threshold (< 8.7%). Similar to the conclusions made within the development of the ANN based model, a higher cut-off value is recommended when applying the model for the prediction of $[M+Na]^+$ ions within DTIMS measurements (see below).

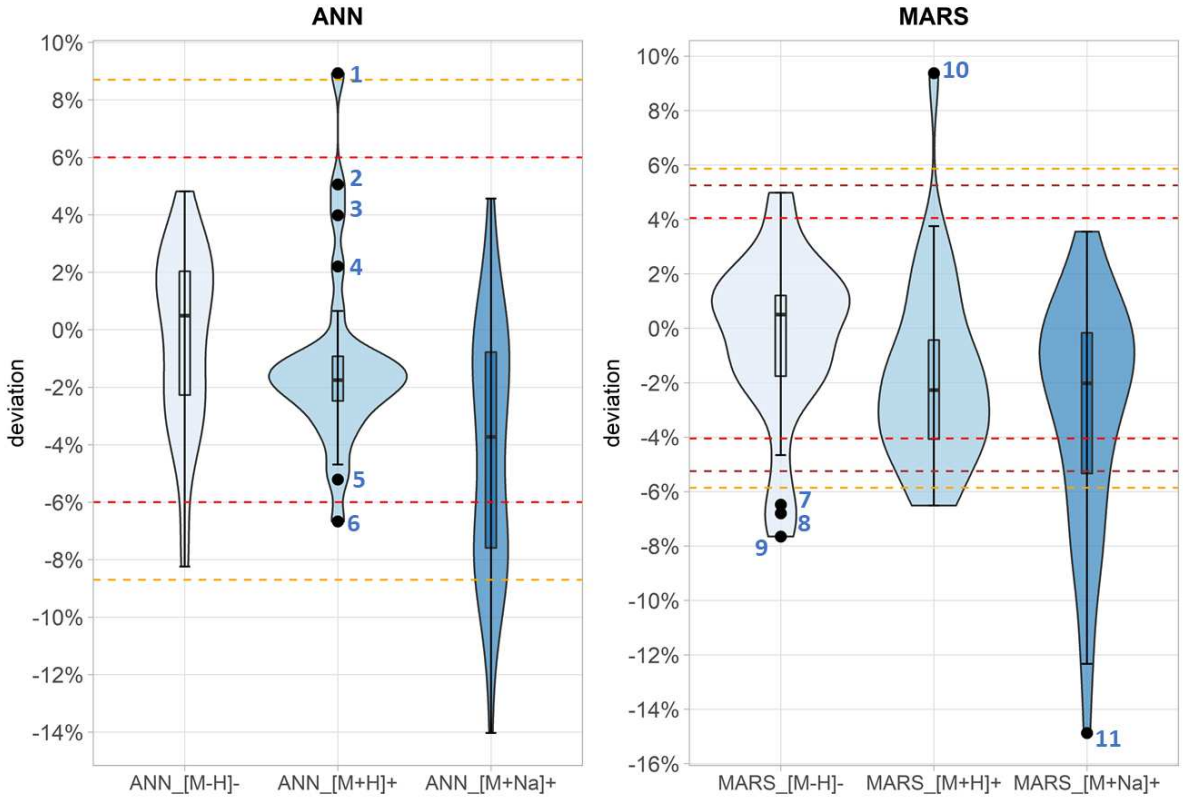

Figure 2: Combined violin and boxplots of the error distributions observed when comparing $^{DT}CCS_{N2}$ values with predicted CCS values deriving from Artificial Neural Network (ANN) and Multivariate Adaptive Regression Splines (MARS) based models. For data in positive ionization polarity, a distinction between proton and sodium adducts is made. The outliers observed for each dataset are numbered as follows: 1: Fyroflex BDP, 2: 5OH-EHDPHP, 3: Fyroflex RDP, 4: TOTP, 5: 4OH-PhP, 6: 5Cl-BTR, 7: 2,4-DEHTM, 8: MEHTP, 9: 5OH-MEHTP, 10: Fyroflex BDP, 11: TOTM. The full names of the mentioned compounds can be found in Table S3. The thresholds applied for the comparisons are indicated with dashed lines. These thresholds are based considering the 95th confidence interval of each model. For the ANN based model, thresholds of 6% ($[M+H]^+$ and $[M-H]^-$ ions; red dashed line) and 8.7% ($[M+Na]^+$; orange dashed line) were applied. MARS based data was compared based on thresholds of 4.1% (red dashed line), 5.9% (orange dashed line) and 5.3% (brown dashed line) for $[M+H]^+$, $[M+Na]^+$ and $[M-H]^-$ ions, respectively.

In contrast to the ANN based prediction model, the MARS based model was validated for all ion species included here (*i.e.,* $[M+H]^+$, $[M+Na]^+$ and $[M-H]^-$ ions). This allowed the reporting of APEs observed for the 95th percentile of the datapoints for each ion species separately [41]. In detail, these APEs corresponded to 4.1%, 5.9% and 5.3% for $[M+H]^+$, $[M-H]^-$ and $[M+Na]^+$ ions, respectively [41], which will be used as thresholds to access the deviations presented in this study.

From the CCS values predicted for $[M+H]^+$ ions applying the MARS based model (further referred to as CCS_{MARS}), 71.9% showed an APE < 4.0%. This corresponds to 9 out of 32 CCS_{MARS} values for $[M+H]^+$ ions showing an APE above the applied threshold. Two of these deviating CCS_{MARS} values were also observed as deviating CCS_{ANN} values, namely BDP (CCS_{MARS} with a deviation of 9.38%) and 5Cl-BTR (CCS_{MARS} with a deviation of -6.52%). Additionally, the CCS_{MARS} values of DIDP, DINP and DINCH showed APEs > 4.0%. The same assumptions as described about the causes of these deviations can be applied here.

For the $[M+Na]^+$ ions, 73.9% of which showed an APE <5.3%, a median deviation of -2.3% and an IQR of 5.2% were observed. This indicates higher (i.e., closer to zero) median values and a smaller IQR than observed for CCS_{ANN} values of sodium adducts. Within the development of the MARS based model, a separate model was developed for the prediction of CCS values of $[M+Na]^+$ ions. Thereby, experimental values of $[M+Na]^+$ adducts were included in the training dataset to account for the higher volume and particularities derived from the allocation of the sodium ion within the molecular structure influencing the shape and size of ions [41]. The lower APEs observed for CCS_{MARS} values of sodium adducts confirm the added value of the described approach indicating that the MARS based model is more suitable for a reliable prediction of CCS values for this ion species. Nevertheless, the APEs reported here still show higher deviations than observed for the comparison with experimental TWIMS based values [41] indicating that additional factors influence the accuracy of the prediction.

For CCS_{MARS} values of $[M-H]^-$ ions, a median deviation of 0.5% and an IQR of 3.0% were observed. 90.0% of the CCS_{MARS} values of $[M-H]^-$ ions showed an APE < 5.9%. This corresponds to 3 out of 30 CCS_{MARS} values with an APE >5.9% which are indicated as outliers in **Figure 2**. Two of the corresponding compounds (MEHTP and 5-HO-MEHTP) had also shown high deviations within their ANN based predicted values. Based on the low number of terephthalates and metabolites included in the dataset, it cannot be stated whether particular structural characteristics or other factors cause the observed high deviations. The same applies to the high deviation observed for the CCS_{MARS} value of the $[M-H]^-$ ion of 2,4-DEHTM (-6.48%).

Table 1: The 95th percentiles observed for the absolute percent errors (APEs) between experimental $^{DT}CCS_{N2}$ values and predicted CCS values. The latter were predicted applying Artificial Neural Network (ANN) and Multivariate Adaptive Regression Splines (MARS) based models.

Ion species	**95th percentile of observed APEs**	
	ANN	**MARS**
$[M+H]^+$	6.08%	6.38%
$[M+Na]^+$	10.29%	11.13%
$[M-H]^-$	5.70%	6.66%

The percentages of ions showing an APE below the applied thresholds are summarized in **Table S9**. Additionally, the 95th percentiles of the absolute percent errors observed for each ion species were calculated (**Table 1**). This aimed at estimating thresholds recommended for future applications of the ANN and MARS based models for DTIMS measurements. From the observed 95th percentiles the conclusion might be drawn that the ANN based model provides better results for DTIMS predictions, as all reported values are lower in comparison to the MARS based model. However, in contrast to the 95th percentiles which were reported within the development of the prediction models[36, 41], the values reported in this study are based on a smaller sample size. Thus, after grouping the

observed APEs by size, the reported 95th percentile is strongly influenced by the data points determining the 95% cut-off. Due to the small percentage range and sample size investigated, even slight deviations of these values towards higher APEs can have strong effects on the calculated percentiles. Especially for $[M+Na]^+$ ions, this approach does not reflect the added advantages of the MARS based model described above, thus not allowing the direct use of the 95th percentiles as proposed thresholds. Nevertheless, the 95th percentiles reported reflect deviations between experimental $^{DT}CCS_{N2}$ values and predicted data which are comparable to the observations reported within the development of the prediction models, thus indicating their applicability for DTIMS measurements. It is recommended to use the reported 95th percentiles in combination with an assessment of possible deviations for the compound class of interest to estimate applicable thresholds. The MARS based model is recommended for the prediction of $[M+Na]^+$ ions[41].

The described considerations indicate the necessity of a critical expert evaluation of the applicability of a prediction model prior to its implementation. The discussion presented here also points out that the various factors influencing both the experimental acquisition and prediction of CCS values do not allow, at this moment, an unsupervised implementation of prediction models and databases acquired on different instrumental set-ups.

3.5 Recommendation of parameters to be reported for CCS prediction models

The acquisition of CCS values represents a measurement of empirical values rather than an absolute and constant physical property. Therefore, a detailed reporting of experimental settings, as well as applied QA measures is crucial to estimate the influence of these parameters on IMS-MS measurements and their reproducibility using other instrumental designs. Parameters recommended to be reported for experimental CCS values have been discussed in detail by Gabelica *et al.* [9] and include mainly mobility device hardware parameters, used drift gas and calibrants or QC compounds. The observed deviations between $^{DT}CCS_{N2}$ and $^{TW}CCS_{N2}$ values described for some of the compound classes investigated in the presented study confirm the necessity of a unified reporting of experimental parameters to trace back possible causes for such findings. Adding to these recommendations, this study proposes a set of parameters recommended to be reported for CCS prediction models in order to highlight their usefulness for other instrumental designs (**Table 2**).

Table 2: Recommended parameters for the reporting of CCS prediction models.

Parameter	Recommended information to report
General	General aim of the development. For which compound classes is the model being developed? Which experimental datasets will be used for the development?

Prediction model	Characteristics of applied prediction model; settings and descriptors used for training of the model
Training set	Detailed information on the identity of compounds used for training of the model; ion species included in the training set; detailed description of experimental parameters used for the acquisition of experimental CCS values used for training of the model
Validation results	Description of results obtained after validating the developed model; description of validation dataset and detailed reporting of results for each ion species. Which thresholds should be applied in future applications of the prediction model?
Inter-lab validation	Evaluation of prediction performance of the model for the particular instrument in use. Study of accuracy of prediction for a small set of molecules to support the decisions on suspect substances.

555

556 **4. CONCLUSIONS**

557 A dataset containing 106 DTIMS derived $^{DT}CCS_{N2}$ values including $[M+H]^+$, $[M+Na]^+$ and $[M-H]^-$ ions
558 was compared with both experimental (TWIMS derived) $^{TW}CCS_{N2}$ values and predicted CCS values.
559 $^{TW}CCS_{N2}$ values were acquired on a VION and Synapt G2 system showing absolute errors < 2% for
560 83% and 82% of the values, respectively, indicating a good reproducibility between different
561 instrumental designs. Moreover, good linear correlations were observed for both systems resulting
562 in correlation coefficients of R^2 = 0.9889 (VION) and R^2 = 0.9929 (Synapt). Nevertheless, deviations of
563 up to -6.55% were observed for a few compounds belonging to particular chemical classes of
564 compounds, Additionally, the applied calibration approaches could not be excluded as a potential
565 cause for the observed deviations. These findings point out that potential biases of experimental
566 databases built on data acquired by a different instrumental set-up, need to be evaluated prior to its
567 implementation.
568 With regards to CCS prediction models, the 95th percentiles of deviations reported for $[M+H]^+$ and
569 $[M-H]^-$ ions between experimental $^{DT}CCS_{N2}$ values and predicted data were comparable to the values
570 reported within the development of the ANN and MARS based models, indicating their applicability
571 for DTIMS measurements. These percentiles can be used to establish thresholds to be applied in
572 future DTIMS based studies. However, different parameters such as the aim and compound class for
573 which the model is developed should be considered prior to its applications.
574

575 **5. ACKNOWLEDGMENTS**

576 L. Belova acknowledges funding through a Research Foundation Flanders (FWO) fellowship
577 (11G1821N). L. Bijlsma acknowledges his fellowship funded by “la Caixa” Foundation. The project
578 that gave rise to these results also received the support of a fellowship from ”la Caixa” Foundation

(ID 10 0 010434). The fellowship code is LCF/BQ/PR21/11840012. Jesse Sterckx is acknowledged for helping with the measurements on the Synapt G2 system. This work received financial support also from the University Jaume I (UJI-B2020-19). The graphical abstract was created with BioRender.com, license no 2641-5211.

6. REFERENCES

[1] L. Mullin, K. Jobst, R.A. DiLorenzo, R. Plumb, E.J. Reiner, L.W.Y. Yeung, I.E. Jogsten, Liquid chromatography-ion mobility-high resolution mass spectrometry for analysis of pollutants in indoor dust: Identification and predictive capabilities, Anal Chim Acta 1125 (2020) 29-40.
[2] A.D. George, M.C.L. Gay, M.E. Wlodek, R.D. Trengove, K. Murray, D.T. Geddes, Untargeted lipidomics using liquid chromatography-ion mobility-mass spectrometry reveals novel triacylglycerides in human milk, Sci Rep 10(1) (2020) 9255.
[3] L. Lacalle-Bergeron, T. Portoles, F.J. Lopez, J.V. Sancho, C. Ortega-Azorin, E.M. Asensio, O. Coltell, D. Corella, Ultra-Performance Liquid Chromatography-Ion Mobility Separation-Quadruple Time-of-Flight MS (UHPLC-IMS-QTOF MS) Metabolomics for Short-Term Biomarker Discovery of Orange Intake: A Randomized, Controlled Crossover Study, Nutrients 12(7) (2020).
[4] T.J. Causon, V. Ivanova-Petropulos, D. Petrusheva, E. Bogeva, S. Hann, Fingerprinting of traditionally produced red wines using liquid chromatography combined with drift tube ion mobility-mass spectrometry, Anal Chim Acta 1052 (2019) 179-189.
[5] J. Hollender, E.L. Schymanski, H.P. Singer, P.L. Ferguson, Nontarget Screening with High Resolution Mass Spectrometry in the Environment: Ready to Go?, Environ Sci Technol 51(20) (2017) 11505-11512.
[6] M. Pourchet, L. Debrauwer, J. Klanova, E.J. Price, A. Covaci, N. Caballero-Casero, H. Oberacher, M. Lamoree, A. Damont, F. Fenaille, J. Vlaanderen, J. Meijer, M. Krauss, D. Sarigiannis, R. Barouki, B. Le Bizec, J.P. Antignac, Suspect and non-targeted screening of chemicals of emerging concern for human biomonitoring, environmental health studies and support to risk assessment: From promises to challenges and harmonisation issues, Environ Int 139 (2020) 105545.
[7] J.W. Lee, Basics of Ion Mobility Mass Spectrometry, Mass Spectrometry Letters 8(4) (2017) 79-89.
[8] V. D'Atri, T. Causon, O. Hernandez-Alba, A. Mutabazi, J.L. Veuthey, S. Cianferani, D. Guillarme, Adding a new separation dimension to MS and LC-MS: What is the utility of ion mobility spectrometry?, J Sep Sci 41(1) (2018) 20-67.
[9] V. Gabelica, A.A. Shvartsburg, C. Afonso, P. Barran, J.L.P. Benesch, C. Bleiholder, M.T. Bowers, A. Bilbao, M.F. Bush, J.L. Campbell, I.D.G. Campuzano, T. Causon, B.H. Clowers, C.S. Creaser, E. De Pauw, J. Far, F. Fernandez-Lima, J.C. Fjeldsted, K. Giles, M. Groessl, C.J. Hogan, Jr., S. Hann, H.I. Kim, R.T. Kurulugama, J.C. May, J.A. McLean, K. Pagel, K. Richardson, M.E. Ridgeway, F. Rosu, F. Sobott, K. Thalassinos, S.J. Valentine, T. Wyttenbach, Recommendations for reporting ion mobility Mass Spectrometry measurements, Mass Spectrom Rev 38(3) (2019) 291-320.
[10] S.M. Stow, T.J. Causon, X. Zheng, R.T. Kurulugama, T. Mairinger, J.C. May, E.E. Rennie, E.S. Baker, R.D. Smith, J.A. McLean, S. Hann, J.C. Fjeldsted, An Interlaboratory Evaluation of Drift Tube Ion Mobility-Mass Spectrometry Collision Cross Section Measurements, Anal Chem 89(17) (2017) 9048-9055.
[11] R.T. Kurulugama, E. Darland, F. Kuhlmann, G. Stafford, J. Fjeldsted, Evaluation of drift gas selection in complex sample analyses using a high performance drift tube ion mobility-QTOF mass spectrometer, Analyst 140(20) (2015) 6834-44.
[12] K. Giles, S.D. Pringle, K.R. Worthington, D. Little, J.L. Wildgoose, R.H. Bateman, Applications of a travelling wave-based radio-frequency-only stacked ring ion guide, Rapid Commun Mass Spectrom 18(20) (2004) 2401-14.
[13] B.T. Ruotolo, J.L. Benesch, A.M. Sandercock, S.-J. Hyung, C.V. Robinson, Ion mobility–mass spectrometry analysis of large protein complexes, Nat Protoc 3(7) (2008) 1139-1152.

627 [14] V. Hinnenkamp, J. Klein, S.W. Meckelmann, P. Balsaa, T.C. Schmidt, O.J. Schmitz, Comparison of
628 CCS Values Determined by Traveling Wave Ion Mobility Mass Spectrometry and Drift Tube Ion
629 Mobility Mass Spectrometry, Anal Chem 90(20) (2018) 12042-12050.
630 [15] A.S. Gelb, R.E. Jarratt, Y. Huang, E.D. Dodds, A study of calibrant selection in measurement of
631 carbohydrate and peptide ion-neutral collision cross sections by traveling wave ion mobility
632 spectrometry, Anal Chem 86(22) (2014) 11396-11402.
633 [16] M.F. Bush, Z. Hall, K. Giles, J. Hoyes, C.V. Robinson, B.T. Ruotolo, Collision cross sections of
634 proteins and their complexes: a calibration framework and database for gas-phase structural
635 biology, Anal Chem 82(22) (2010) 9557-9565.
636 [17] V. Gabelica, E. Marklund, Fundamentals of ion mobility spectrometry, Curr Opin Chem Biol 42
637 (2018) 51-59.
638 [18] T.O. Metz, E.S. Baker, E.L. Schymanski, R.S. Renslow, D.G. Thomas, T.J. Causon, I.K. Webb, S.
639 Hann, R.D. Smith, J.G. Teeguarden, Integrating ion mobility spectrometry into mass spectrometry-
640 based exposome measurements: what can it add and how far can it go?, Bioanalysis 9(1) (2017) 81-
641 98.
642 [19] A. Celma, L. Ahrens, P. Gago-Ferrero, F. Hernandez, F. Lopez, J. Lundqvist, E. Pitarch, J.V. Sancho,
643 K. Wiberg, L. Bijlsma, The relevant role of ion mobility separation in LC-HRMS based screening
644 strategies for contaminants of emerging concern in the aquatic environment, Chemosphere 280
645 (2021) 130799.
646 [20] L. Belova, N. Caballero-Casero, A.L.N. van Nuijs, A. Covaci, Ion Mobility-High-Resolution Mass
647 Spectrometry (IM-HRMS) for the Analysis of Contaminants of Emerging Concern (CECs): Database
648 Compilation and Application to Urine Samples, Anal Chem 93(16) (2021) 6428-6436.
649 [21] A. Celma, J.V. Sancho, E.L. Schymanski, D. Fabregat-Safont, M. Ibanez, J. Goshawk, G.
650 Barknowitz, F. Hernandez, L. Bijlsma, Improving Target and Suspect Screening High-Resolution Mass
651 Spectrometry Workflows in Environmental Analysis by Ion Mobility Separation, Environ Sci Technol
652 54(23) (2020) 15120-15131.
653 [22] L. Bijlsma, R. Bade, F. Been, A. Celma, S. Castiglioni, Perspectives and challenges associated with
654 the determination of new psychoactive substances in urine and wastewater–A tutorial, Anal Chim
655 Acta 1145 (2021) 132-147.
656 [23] J.N. Dodds, Z.R. Hopkins, D.R.U. Knappe, E.S. Baker, Rapid Characterization of Per- and
657 Polyfluoroalkyl Substances (PFAS) by Ion Mobility Spectrometry-Mass Spectrometry (IMS-MS), Anal
658 Chem 92(6) (2020) 4427-4435.
659 [24] S. Goscinny, M. McCullagh, J. Far, E. De Pauw, G. Eppe, Towards the use of ion mobility mass
660 spectrometry derived collision cross section as a screening approach for unambiguous identification
661 of targeted pesticides in food, Rapid Commun Mass Spectrom 33 (2019) 34-48.
662 [25] E. Canellas, P. Vera, C. Nerin, Ion mobility quadrupole time-of-flight mass spectrometry for the
663 identification of non-intentionally added substances in UV varnishes applied on food contact
664 materials. A safety by design study, Talanta 205 (2019) 120103.
665 [26] K.M. Hines, J. Herron, L. Xu, Assessment of altered lipid homeostasis by HILIC-ion mobility-mass
666 spectrometry-based lipidomics, J. Lipid Res. 58(4) (2017) 809-819.
667 [27] X. Zheng, N.A. Aly, Y. Zhou, K.T. Dupuis, A. Bilbao, V.L. Paurus, D.J. Orton, R. Wilson, S.H. Payne,
668 R.D. Smith, A structural examination and collision cross section database for over 500 metabolites
669 and xenobiotics using drift tube ion mobility spectrometry, Chemical science 8(11) (2017) 7724-
670 7736.
671 [28] M. Hernandez-Mesa, B. Le Bizec, F. Monteau, A.M. Garcia-Campana, G. Dervilly-Pinel, Collision
672 Cross Section (CCS) Database: An Additional Measure to Characterize Steroids, Anal Chem 90(7)
673 (2018) 4616-4625.
674 [29] D.H. Ross, J.H. Cho, L. Xu, Breaking down structural diversity for comprehensive prediction of
675 ion-neutral collision cross sections, Anal Chem 92(6) (2020) 4548-4557.

[30] J.A. Picache, B.S. Rose, A. Balinski, K.L. Leaptrot, S.D. Sherrod, J.C. May, J.A. McLean, Collision cross section compendium to annotate and predict multi-omic compound identities, Chem Sci 10(4) (2019) 983-993.
[31] Z. Zhou, X. Shen, J. Tu, Z.J. Zhu, Large-Scale Prediction of Collision Cross-Section Values for Metabolites in Ion Mobility-Mass Spectrometry, Anal Chem 88(22) (2016) 11084-11091.
[32] Z. Zhou, M. Luo, X. Chen, Y. Yin, X. Xiong, R. Wang, Z.J. Zhu, Ion mobility collision cross-section atlas for known and unknown metabolite annotation in untargeted metabolomics, Nat Commun 11(1) (2020) 4334.
[33] Z. Zhou, J. Tu, X. Xiong, X. Shen, Z.J. Zhu, LipidCCS: Prediction of Collision Cross-Section Values for Lipids with High Precision To Support Ion Mobility-Mass Spectrometry-Based Lipidomics, Anal Chem 89(17) (2017) 9559-9566.
[34] C.B. Mollerup, M. Mardal, P.W. Dalsgaard, K. Linnet, L.P. Barron, Prediction of collision cross section and retention time for broad scope screening in gradient reversed-phase liquid chromatography-ion mobility-high resolution accurate mass spectrometry, J. of Chrom A 1542 (2018) 82-88.
[35] S.M. Colby, D.G. Thomas, J.R. Nunez, D.J. Baxter, K.R. Glaesemann, J.M. Brown, M.A. Pirrung, N. Govind, J.G. Teeguarden, T.O. Metz, R.S. Renslow, ISiCLE: A Quantum Chemistry Pipeline for Establishing in Silico Collision Cross Section Libraries, Anal Chem 91(7) (2019) 4346-4356.
[36] L. Bijlsma, R. Bade, A. Celma, L. Mullin, G. Cleland, S. Stead, F. Hernandez, J.V. Sancho, Prediction of Collision Cross-Section Values for Small Molecules: Application to Pesticide Residue Analysis, Anal Chem 89(12) (2017) 6583-6589.
[37] L. Bijlsma, M.H. Berntssen, S. Merel, A refined nontarget workflow for the investigation of metabolites through the prioritization by in silico prediction tools, Anal Chem 91(9) (2019) 6321-6328.
[38] D. Fabregat-Safont, M. Ibáñez, L. Bijlsma, F. Hernández, A.V. Waichman, R. de Oliveira, A. Rico, Wide-scope screening of pharmaceuticals, illicit drugs and their metabolites in the Amazon River, Water Research 200 (2021) 117251.
[39] T.J. Causon, S. Hann, Uncertainty Estimations for Collision Cross Section Determination via Uniform Field Drift Tube-Ion Mobility-Mass Spectrometry, J Am Soc Mass Spectrom 31(10) (2020) 2102-2110.
[40] L. Righetti, N. Dreolin, A. Celma, M. McCullagh, G. Barknowitz, J.V. Sancho, C. Dall'Asta, Travelling Wave Ion Mobility-Derived Collision Cross Section for Mycotoxins: Investigating Interlaboratory and Interplatform Reproducibility, J Agric Food Chem 68(39) (2020) 10937-10943.
[41] A. Celma, R. Bade, J.V. Sancho, F. Hernández, M. Humpries, L. Bijlsma, Prediction of Retention Time and Collision Cross Section (CCSH+ , CCSH- and CCSNa+) of emerging contaminants using Multiple Adaptive Regression Splines. Preprint at https://doi.org/10.21203/rs.3.rs-1249834/v1. Tool available at: https://datascience-adelaideuniversity.shinyapps.io/Predicting_RT_and_CCS/, (2022).
[42] I. Campuzano, M.F. Bush, C.V. Robinson, C. Beaumont, K. Richardson, H. Kim, H.I. Kim, Structural characterization of drug-like compounds by ion mobility mass spectrometry: comparison of theoretical and experimentally derived nitrogen collision cross sections, Anal Chem 84(2) (2012) 1026-1033.
[43] M.F. Bush, I.D. Campuzano, C.V. Robinson, Ion mobility mass spectrometry of peptide ions: effects of drift gas and calibration strategies, Anal Chem 84(16) (2012) 7124-7130.
[44] I. Sushko, S. Novotarskyi, R. Körner, A.K. Pandey, M. Rupp, W. Teetz, S. Brandmaier, A. Abdelaziz, V.V. Prokopenko, V.Y. Tanchuk, Online chemical modeling environment (OCHEM): web platform for data storage, model development and publishing of chemical information, J. Comput Aid Mol Des 25(6) (2011) 533-554.
[45] P.L. Plante, E. Francovic-Fontaine, J.C. May, J.A. McLean, E.S. Baker, F. Laviolette, M. Marchand, J. Corbeil, Predicting Ion Mobility Collision Cross-Sections Using a Deep Neural Network: DeepCCS, Anal Chem 91(8) (2019) 5191-5199.

[46] K.M. Hines, J.C. May, J.A. McLean, L. Xu, Evaluation of collision cross section calibrants for structural analysis of lipids by traveling wave ion mobility-mass spectrometry, Analytical chemistry 88(14) (2016) 7329-7336.
[47] M.L. Feuerstein, M. Hernández-Mesa, Y. Valadbeigi, B. Le Bizec, S. Hann, G. Dervilly, T. Causon, Critical evaluation of the role of external calibration strategies for IM-MS, Analytical and Bioanalytical Chemistry (2022) 1-11.